Walisongo Journal of Chemistry
Walisongo Journal of Chemistry Vol. 9 Issue 1 (2026), 1-14
ISSN: 2621-5985 (online); 2549-385X (print)
DOI: https://doi.org/10.21580/wjc.v9i1.28570

ISOLATION AND CHARACTERIZATION OF β-SITOSTEROL FROM *ACANTHOSTRONGYLOPHORA INGENS* SPONGE AND ITS ANTICANCER ACTIVITY USING AN *IN SILICO* APPROACH

Ajuk Sapar[1*], Riska Mardiyanti[1], Nur Asmi[1], Nunuk Hariani Soekamto[1], Millenia[2], Nurmasyita[1], Nurmalah Syam[1]

[1]Department of Chemistry, Faculty of Mathematics and Natural Sciences, Universitas Hasanuddin, Makassar, Indonesia
[2]Department of Chemistry, Faculty of Mathematics and Natural Sciences, Universitas Tanjungpura, Pontianak, Indonesia

*Corresponding author: ajuksapar@unhas.ac.id

Abstract

This study reports the isolation of β-sitosterol from the methanol extract of the sponge Acanthostrongylophora ingens*, collected from the Spermonde Islands. The methods employed in this study included extraction, phytochemical testing, toxicity assessment, and chromatographic fractionation. Characterization of the isolate was performed using FTIR and GC-MS techniques. Isolate I-3 showed characteristic absorption bands corresponding to functional groups associated with β-sitosterol, and its molecular mass was confirmed at 414 g/mol. The potential anticancer activity was evaluated using an* in silico *approach. The toxicity test results indicated that the methanol extract exhibited high toxicity, with an LC_{50} value of 24.831 µg/mL. Furthermore, the* in silico *molecular docking analysis d emonstrated a strong interaction between β-sitosterol and the target protein, with the lowest binding energy recorded at −11.49 kcal/mol. This significant value suggests that β-sitosterol has excellent interaction potential with the active site of the target protein, highlighting its promising candidacy as an anticancer agent.*

Keywords: *Acanthostrongylophora ingens; sponge; β-Sitosterol; in silico; anticancer*

Introduction

The sponge *Acanthostrongylophora ingens* is a species belonging to the class Demospongiae and is known to contain secondary metabolites with antibacterial [1,2], anticancer [2], and cytotoxic activities. This species is also distributed in Indonesian waters, including the Spermonde Islands. Various secondary metabolites have been identified from *A. ingens*, including alkaloids, steroids, and phenolics. Several alkaloid compounds from *A. ingens*, such as halicyclamine derivatives and diketopiperazines, exhibit antibacterial activity [3]. In addition, four β-carboline alkaloid compounds, namely 1,2,3,4-tetrahydronorharman-1-one, acanthomine A, annomontine, and ingenine E, have shown the most potent cytotoxicity [4]. Steroid compounds have also been found in sponges with various molecular frameworks, such as manadosterols A and B from the sponge *Lissodendryx fibrosa* [5] and β-sitosterol from *Haliclona* sp. [6]. β-Sitosterol is known to have potential as a

chemopreventive agent against breast cancer [7]. Therefore, given the presence of β-sitosterol in the sponge species *A. ingens* in this study, further exploration of its potential and activity through an *in silico* approach is necessary. Through *in silico* studies, information can be obtained regarding whether steroid compounds have the potential to be developed as anticancer drugs.

Experimental Section

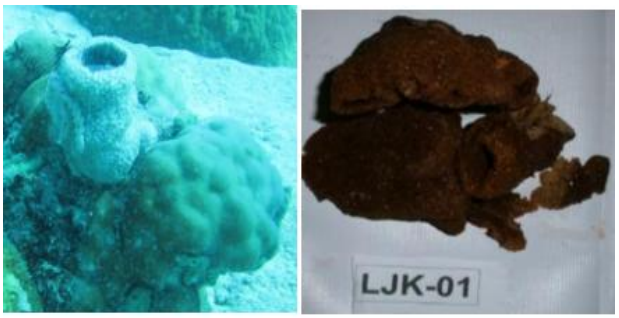

a). b)

Figure 1. Sponge sample photograph: (a) underwater and (b) exposed on the surface.

Materials

The research materials included marine animal samples, namely sponges collected from the waters of Lanjukkang Island, with the code number O1 (LJK-01), by hand using SCUBA diving equipment at a depth of 5 m. Documentation of the sponge was carried out underwater and above the surface. The color of the sponge underwater was dark blue (see Figure 1a), whereas after some time on the surface, it changed to brownish blue (see Figure 1b). This color change occurred because the body parts of this sponge species underwent oxidation in response to the surrounding environment. Other materials used were methanol p.a. (Merck), n-hexane p.a. (Merck), dichloromethane p.a. or DCM (Merck), ethyl acetate p.a. or EA (Merck), cerium sulfate p.a. (Merck), Kieselgel G60 (Merck), thin-layer chromatography plates, aluminum plate, 20 × 20 cm, silica F254, Merck, Dragendorff's reagent, Mayer's reagent, Wagner's reagent, Liebermann–Burchard reagent, Salkowski reagent, $FeCl_3$, and filter paper (Whatman No. 41).

Instruments

The instruments used included analytical balances (Mettler AE 100 and PM200), a melting point apparatus, a rotary evaporator (Heidolph 4000), an FTIR spectrophotometer (Shimadzu Prestige-21), and GC-MS instruments, namely GC-Thermo Scientific Trace 1310-ISQ7000 and MS-Thermo ISQ Series.

Procedure

This research was conducted in several stages, including extraction and partitioning, phytochemical tests, toxicity tests, fractionation and chromatography, FTIR analysis, GC-MS analysis, and *in silico* analysis.

Extraction: maceration and partitioning

A total of 587.5 g of wet *A. ingens* sponge (see Figure 1) was extracted using the maceration technique with 3 × 1200 mL of methanol p.a. The extraction product was then filtered using Whatman No. 41 filter paper. Next, the methanol solvent in the filtrate was evaporated using a rotary evaporator to obtain the LJK-01 methanol

extract. Not all of the methanol extract was subjected to the partitioning stage; some was used for toxicity testing and TLC analysis. The methanol extract was then partitioned sequentially using three solvents of different polarities: *n*-hexane, dichloromethane (DCM), and ethyl acetate (EA). Before partitioning, the concentrated methanol extract was suspended in 5% distilled water in methanol. The partitioning process was then continued using *n*-hexane for 6 × 24 h, resulting in the *n*-hexane extract, which was subsequently evaporated using a rotary evaporator to obtain the concentrated *n*-hexane extract. The methanol-water portion was then partitioned using DCM for 6 × 24 h to obtain the DCM extract. Finally, the methanol-water portion was partitioned using ethyl acetate for 6 × 24 h to obtain the ethyl acetate extract and residue.

Phytochemical tests

For the alkaloid test, the methanol, *n*-hexane, DCM, and ethyl acetate extracts of *A. ingens* sponge were placed in separate test tubes and reacted with Dragendorff's, Mayer's, and Wagner's reagents. A positive result for alkaloids was indicated by the formation of an orange color with Dragendorff's reagent, a white color with Mayer's reagent, and a brown color with Wagner's reagent. For the steroid test, the sample was reacted with Liebermann–Burchard reagent, which produces a bluish-green color in the presence of steroids. For the terpenoid test, Salkowski reagent was used. In this test, the sample dissolved in chloroform was reacted with sulfuric acid, resulting in the formation of a red or brown ring at the bottom layer. For the phenolic content test, the sample was reacted with $FeCl_3$, producing a dark purple to black color.

Toxicity test

The toxicity test of the methanol extract was conducted using *Artemia salina* larvae through the brine shrimp lethality test (BSLT) method [8]. The methanol extract was prepared in triplicate at concentrations of 1000, 100, and 10 ppm, along with a control solution. Each test container was then filled with 10 *A. salina* larvae, including the control group. Observations were conducted for 24 h by counting the number of dead larvae, and the LC_{50} value was calculated using probit analysis.

Fractionation

Fractionation was performed using silica gel G60 F254 by vacuum column chromatography (VCC) with Kieselgel G60. The column chromatography fractions were collected in 100 mL bottles and examined by TLC under a UV lamp, followed by visualization with cerium sulfate reagent. Fractions showing similar spots were combined and then evaporated to obtain dry or viscous isolates. Purification was carried out by recrystallization and monitored using two-dimensional TLC with two to three solvent systems, as well as melting point analysis, until the melting point range did not exceed 2°C.

FTIR Analysis

Isolate sample I-3 was placed in an oven to remove water and then ground with KBr. The mixture was pressed into pellets and placed in the FTIR sample holder. FTIR measurements were then performed.

GC-MS Analysis

GC-MS analysis of isolate I-3 was performed using GC-Thermo Scientific Trace 1310-ISQ7000 and MS-Thermo ISQ Series instruments with the following column characteristics: column type, TG-5MS; column length, 30 m; column diameter, 0.25 mm; and film thickness, 0.25 µm. The method type used was a general acquisition method to acquire all data types. The MS transfer line temperature was 250°C, the ion source temperature was

200°C, and the ionization mode was electron impact (EI). The retention time was 30 min, with a programmed temperature range of 70–250°C.

In Silico *Analysis*

a. Analysis of Lipinski's Rule and ADMET

Lipinski's rule was used to assess the stability and physicochemical properties of compounds related to oral membrane permeability, while ADMET analysis was used to predict pharmacokinetic and toxicity profiles [9], [10]. Compounds obtained from the GC-MS results of *A. ingens* were modeled in 3D and then converted into .smile file format using the Open Babel GUI application. Files in SMILES format for Lipinski's rule evaluation were uploaded to the SwissADME online platform (http://www.swissadme.ch/). The run button was then pressed to obtain Lipinski's rule parameter data. For ADMET analysis, the files were uploaded to the pkCSM online platform (https://biosig.lab.uq.edu.au/pkcsm/prediction). The ADMET button was then pressed to obtain absorption, distribution, metabolism, excretion, and toxicity data [11],[12]. The combination of Lipinski and ADMET analyses provides a comprehensive approach in the early stages of drug selection, ensuring that compounds are not only biologically active but also possess favorable pharmacological characteristics [13, 14].

b. Molecular Docking Analysis

The macromolecule used was the EGFR receptor complex, downloaded from the Protein Data Bank (PDB) with the PDB ID 3OLL (https://www.rcsb.org/structure). Docking preparation included hydrogen addition, charge addition, and residue removal from the protein structure using the Dock Prep menu in Chimera software. Docking was performed using a grid-based docking method with a flexible ligand–rigid receptor approach. This method allows efficient evaluation of ligand binding energies at the protein active site while maintaining structural stability and ligand conformational flexibility [15]. The molecular docking process was carried out using AutoDock 4.2 with the assistance of AutoDockTools [16]. Protein and ligand preparations were saved in .pdb format files. Each ligand was docked to the active site of the protein. Docking parameters were created by setting the grid box size to 40 × 40 × 40 Å, centered on the ligand, with a spacing of 0.375 Å, and then saved in .gpf format [17]. Each ligand was set to produce 10 conformations using the Lamarckian genetic algorithm, and the best conformation was selected based on the lowest binding energy. Validation of the docking process was determined by observing the RMSD value of the standard ligand after redocking, with an acceptable value of no more than 2 Å. The docking results were visualized using Discovery Studio Visualizer software [18].

Results and Discussion

Extraction: maceration and partitioning

Extraction of 587.5 g of wet *A. ingens* sponge using methanol p.a. yielded 0.8305 g of concentrated methanol extract. Furthermore, partitioning using *n*-hexane, dichloromethane, and ethyl acetate produced fractions weighing 197.9 mg, 282.7 mg, and 53.1 mg, respectively, while the residual weight after evaporation was 155.8 mg. The extraction and partitioning results are presented in Table 1.

Table 1. Weight and yield data from extraction and partitioning

No.	Extract Type/Fraction	Weight (g/mg)	Yield (%)
1.	Methanol extract	0.8305 g	-
2.	*n*-Hexane fraction	197.9 mg	23.8
3.	DCM fraction	282.7 mg	34.0
4.	Ethyl acetate fraction	53.1 mg	6.4

5.	Residue	155.8 mg	18.8

Phytochemical test

The results of the phytochemical tests on the methanol extract, *n*-hexane fraction, DCM fraction, ethyl acetate fraction, and methanol-water residue using several specific reagents are shown in Table 2. Wagner's, Mayer's, and Dragendorff's reagents were used to detect alkaloids, Liebermann–Burchard reagent was used to detect steroids, Salkowski reagent was used to detect terpenoids, and $FeCl_3$ was used to detect phenolic compounds.

Table 2. Results of phytochemical tests of extracts and fractions

No	Sample Code	Dragendorff's Reagent	Wagner's Reagent	Mayer's Reagent	Terpene	Steroid	Phenolic
1	E-Methanol	+++	++	++	+	+++	+
2	FH	-	-	-	++	+++	_
3	FD	++	+	++	+	++	+
4	FEA	+	-	+	-	-	+
5	Residue	+	-	+	-	-	+

Notes:
Response: +++ = strong; ++ = moderate; + = weak; - = no response.
FH = *n*-hexane fraction; FD = dichloromethane fraction; FEA = ethyl acetate fraction.

Toxicity test

Toxicity testing is a preliminary assay used to determine the potential of an extract as an anticancer agent. Toxicity testing was performed on the LJK-01 methanol extract using the Brine Shrimp Lethality Test (BSLT) method. The test results are shown in Table 3. The toxicity test results showed that the LC_{50} value of the LJK-01 methanol extract was 24.831 µg/mL, indicating strong toxicity. Therefore, the methanol extract of LJK-01 has the potential to be further investigated for active secondary metabolites through cytotoxicity testing using MCF-7 cancer cells.

Table 3. Observation data on the lethality of *A. salina* Leach after 24 h for the sponge sample *A. ingens*

Sample Code	Number of Dead Larvae per Concentration			Percentage of Larval Mortality (%)			Larval Mortality (%) after Control Correction		
	10 ppm	10 ppm	10 ppm	100 ppm	1000 ppm	100 ppm	1000 ppm	100 ppm	1000 ppm
LJK-01	6	5	10						
	5	5	10						
	5	4	10						
Total mortality	16	14	30	53	47	100	27	30	60
24.83 (µg/mL)									

Fractionation

Fractionation was performed on the partitioned *n*-hexane extract. The *n*-hexane fraction was selected to obtain information on secondary metabolites contained in the non-polar fraction, particularly steroid compounds. Separation of secondary metabolites from the *n*-hexane fraction using CVC resulted in 19 fractions from gradient elution, with eluent compositions ranging from 100% *n*-hexane, *n*-hexane:DCM, 100% DCM, DCM:methanol, and 100% methanol. TLC analysis of the 19 fractions yielded five combined fractions based on their spot patterns.

The FG-3 fraction was selected because it had the largest major spot and the highest mass, 61 mg, and its Rf value matched that of the β-sitosterol standard. FG-3 was then recrystallized using hot methanol, and methanol-insoluble impurities were removed by filtration. The filtrate was cooled to form 32 mg of crystals, FG-3C, which were separated from the mother liquor, FG-3P. FG-3C was washed with a small amount of cold solvent and allowed to dry. Both isolates and the standard were eluted on TLC using an eluent composition of *n*-hexane:DCM, 4:6. The TLC results for both isolates are shown in Figure 2. Further purification of FG-3C using preparative thin-layer chromatography (PTLC) yielded five isolates, I-1 to I-5, as shown in Figure 3. Spots I-2 and I-3 had nearly identical Rf values of 0.12 in the eluent composition *n*-hexane:DCM, 5:5, and differed from the other spots.

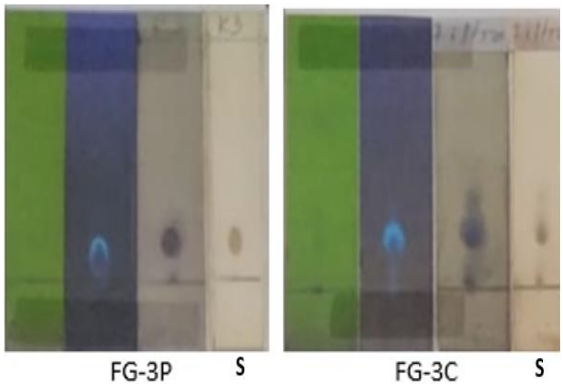

Figure 2. TLC results of FG-3P, FG-3C, and S, the β-sitosterol standard.

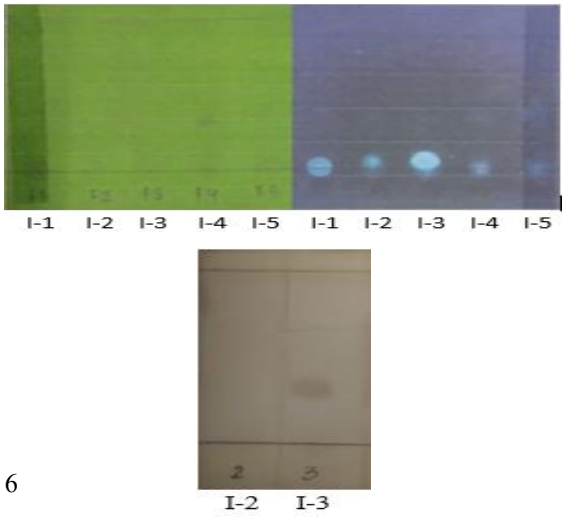

Figure 3. TLC results of five isolates obtained from preparative thin-layer chromatography (PTLC).

Subsequently, the two spots, I-2 and I-3, were re-eluted and reacted with cerium sulfate as a spot-detecting reagent. I-3 showed a major spot that changed from orange to brown upon heating, as is typical of β-sitosterol spots (see Figure 3). Therefore, I-3 was selected for the characterization stage, including FTIR and GC-MS analyses, as well as *in silico* testing.

FTIR Analysis

The FTIR analysis results of isolate I-3 are shown in Figure 4. The interpretation of the FTIR spectrum is presented in Table 4. The functional groups identified at each wavenumber are closely associated with steroid compounds, particularly β-sitosterol, as indicated by comparison with the TLC standard. The functional groups O-H, C-O, C=C, =C-H, and C-H are present in β-sitosterol. In addition, C=O, O-H, C-O, and C-H functional groups are associated with fatty acids.

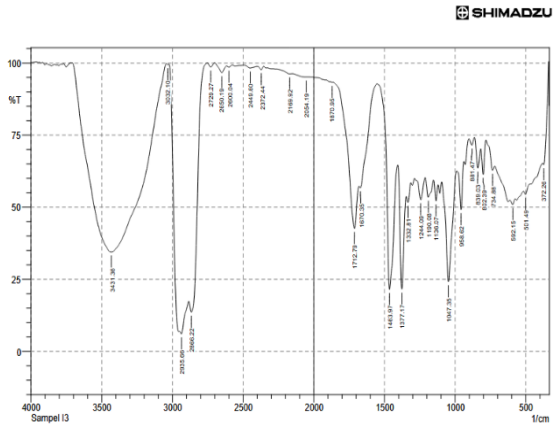

Figure 4. FTIR spectrum of isolate I-3.

Table 4. Interpretation of the FTIR spectrum of isolate I-3

Functional Group	Wavenumber (cm^{-1})
O-H *stretching*	3431.36
=C-H *stretching*	3032.10
C-H *stretching*	2935.66 and 2866.22
C-H *bending*	1463.97 and 1377.17
C=O *stretching*	1712.79
C=C *stretching*	1670.35

C-O *stretching*	1047.35 and 1136.07

GC-MS analysis

The GC analysis results are shown in Figure 5. Based on the phytochemical and TLC test results, I-3 was identified as a steroid compound, namely β-sitosterol, with the molecular formula $C_{29}H_{50}O$ and a molecular weight of 414.718 g/mol. This finding is in good agreement with the MS results from the GC-MS analysis, as shown in Figure 6. Six selected compounds were identified based on their library similarity, as shown in Table 5.

Table 5. Six selected compounds identified by GC-MS

No.	Compound Name	T_r	Relative Area (%)	Relative Similarity Index
1	*n*-Hexadecanoic acid	19.965	6.17	88.6
2	9,12-Octadecadienoic acid (Z,Z)-, methyl ester	21.570	2.73	90.0
3	9-Octadecenoic acid (Z)-, methyl ester	21.641	4.64	94.0
4	trans-13-Octadecenoic acid	22.199	5.72	90.0
5	cis-Vaccenic acid	22.237	7.70	88.5
6	β-Sitosterol	25.029	0.55	84.7

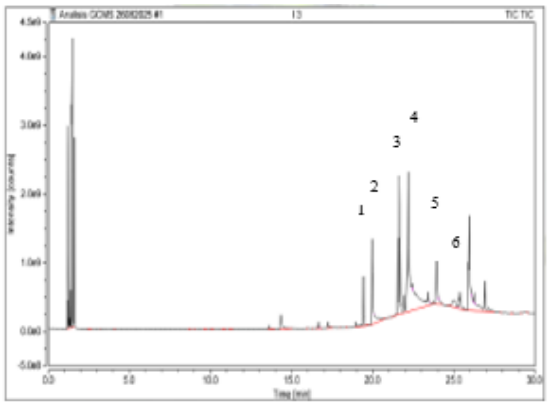

Figure 5. GC chromatogram of I-3.

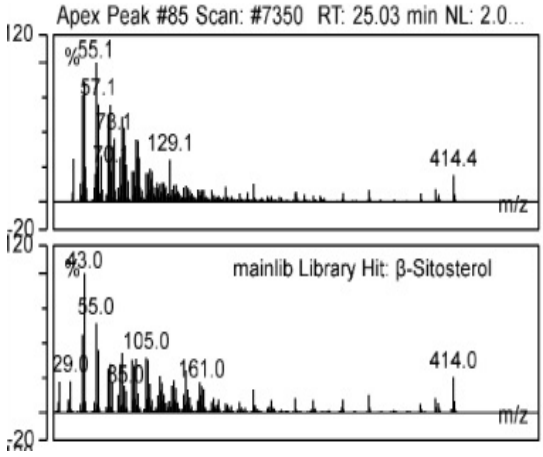

Figure 6. MS spectrum of β-sitosterol.

In silico *analysis*

Lipinski's rule and ADMET analysis

In silico analysis of three identified compounds from *A. ingens*, namely β-sitosterol, cis-vaccenic acid, and *n*-hexadecanoic acid, revealed distinct profiles and provided relevant pharmacokinetic implications for their development as anticancer agents. *In silico* predictions indicate antioxidant potential associated with anticancer activity for one of the possible compounds, namely *n*-hexadecanoic acid [19]. Evaluation using Lipinski's criteria (see Table 6), including molecular weight <500 g/mol, H-bond donors ≤5, H-bond acceptors ≤10, and Log P ≤5, as well as flexibility parameters, such as the number of freely rotating bonds, provided an overview of the priorities and optimization needs for each compound.

Table 6. Lipinski's rule

Compound	Molecular Weight (g/mol)	H-Bond Acceptors	H-Bond Donors	No. of Rotatable Bonds	Log P
1	414.71	1	1	6	6.73
2	282.46	2	1	15	4.57
3	256.42	2	1	14	4.19

In silico analysis of the three key compounds from *A. ingens* showed that all compounds generally met Lipinski's criteria in terms of molecular weight, <500 g/mol, and the number of hydrogen bond donors

and acceptors, thus predicting good oral absorption. Although lipophilicity supports membrane permeability, formulation approaches or structural modifications are needed to reduce pharmacokinetic risks [20]. Furthermore, all three compounds exhibited a high number of freely rotating bonds, ≥6 and up to 15, reflecting significant conformational flexibility. According to Lipinski's rule, a molecule is likely to be orally inactive if it violates two or more of the four rules [21]. The analysis showed that most of the compounds have molecular characteristics suitable for development as drug candidates. This supports the potential of compounds in *A. ingens* to act as anticancer agents, which can be further optimized through structural or formulation modifications. Absorption, distribution, metabolism, excretion, and toxicity (ADMET) analysis was performed to predict the pharmacokinetic behavior and safety of the three bioactive compounds identified in *A. ingens*. The ADMET predictions in Table 7 indicated that all compounds had good oral absorption potential, as evidenced by their relatively high Caco-2 permeability values and human intestinal absorption (HIA) values, ranging from 90% to 96%. This indicates the possibility of adequate bioavailability if the compounds are formulated appropriately. However, all three compounds showed low aqueous solubility, ranging from −5.5 to −6.9, which may represent a major obstacle to actual absorption. This condition highlights the importance of developing formulation strategies, such as the use of solubility enhancers or nanoformulation techniques, to improve the solubility of these compounds [14].

Table 7. ADMET prediction

rediction	**Model Name**	**Compound**		
		1	**2**	**3**
bsorption	Water solubility	-6.957	-5.924	-5.562
	Caco-2 permeability	1.267	1.563	1.558
	Human intestinal absorption	95.884	91.823	92.004
	Skin permeability	-2.705	-2.725	-2.717
	P-glycoprotein substrate	No	No	No
	P-glycoprotein I inhibitor	Yes	No	No
	P-glycoprotein II inhibitor	Yes	No	No
istribution	VDss, human	0.12	-0.558	-0.543
	Fraction unbound, human	0	0.052	0.101
	BBB permeability	0.824	-0.168	-0.111
	CNS permeability	-1.379	-1.654	-1.816
letabolism	CYP2D6 substrate	No	No	No
	CYP3A4 substrate	Yes	Yes	Yes
	CYP1A2 inhibitor	No	Yes	No
	CYP2C19 inhibitor	No	No	No
	CYP2C9 inhibitor	No	No	No
	CYP2D6 inhibitor	No	No	No
	CYP3A4 inhibitor	No	No	No
xcretion	Total clearance	0.628	1.883	1.763
	Renal OCT2 substrate	No	No	No
oxicity	AMES toxicity	No	No	No
	Maximum tolerated dose	-0.341	-0.81	-0.708

hERG I inhibitor	No	No	No
hERG II inhibitor	Yes	No	No
Oral rat acute toxicity	2.854	1.417	1.44
Oral rat chronic toxicity	1.085	3.259	3.181
Hepatotoxicity	No	No	No
Skin sensitization	No	Yes	Yes
T. pyriformis toxicity	0.477	0.676	0.84
Minnow toxicity	-2.079	-1.438	-1.083

Regarding metabolism, there was no strong indication that these compounds act as major CYP enzyme inhibitors. However, there is a possibility of metabolism via the CYP3A4 pathway; therefore, the risk of presystemic metabolism should still be considered. Meanwhile, the excretion profiles indicated that the compounds had variable clearance rates, with no indication of being substrates for the renal transporter OCT2. Thus, renal elimination is not expected to be a major pathway [20]. In terms of toxicity, the prediction results indicated that all compounds were non-mutagenic, as shown by negative AMES test results, and non-hepatotoxic, which are initial indications of safety. However, some compounds were predicted to have potential skin sensitization effects and hERG II channel inhibition, indicating the need for experimental confirmation of possible cardiotoxic effects. Overall, these ADMET results provide positive indications of the compounds' suitability as drug candidates, particularly in terms of absorption and initial safety. However, challenges such as low solubility, potential metabolic interactions, and possible cardiotoxic side effects require further investigation.

Molecular docking analysis is a method used to predict the activity of a compound against a specific protein based on its binding energy [22]. The three major compounds of *A. ingens* were used as ligands and then compared with the native ligand. The native ligand, estradiol, found in the PDB structure 3OLL, was used as a control ligand for validation and comparison in the docking analysis. This ligand represents the natural binding position in the EGFR active site and was used to assess the suitability of the ligand position in the docking results. Validation of the docking method was performed by observing the root-mean-square deviation (RMSD) value. An RMSD value of <2 Å indicates that the native ligand conformation obtained through redocking is close to the test conformation used for molecular docking analysis [23]. The molecular docking results in Table 8 are expressed as binding energy values and provide an overview of the effectiveness of the interaction between the ligand and the protein.

Based on the binding energies obtained, β-sitosterol exhibited the lowest value, at −11.49 kcal/mol, indicating the strongest binding affinity among all ligands and even stronger than that of the native ligand, which had a binding energy of −9.62 kcal/mol. This value indicates that β-sitosterol has excellent interaction potential with the protein active site, likely driven by its lipophilic nature and ability to form extensive hydrophobic interactions. The more negative binding energy value of β-sitosterol compared with that of the native ligand suggests the possibility of stable and specific binding, making this compound a promising candidate for anticancer activity.

Table 8. Molecular Docking Results of Three Compounds from *A. ingens*

No	Ligand	Binding Energy (kcal/mol)
1	β-Sitosterol	-11.49
2	cis-Vaccenic acid	-4.57
3	Hexadecanoic acid	-4.88

4	Native ligand	-9.62

The compounds cis-vaccenic acid and hexadecanoic acid exhibited binding energies of −4.57 kcal/mol and −4.88 kcal/mol, respectively, which were much higher, or less negative, than those of β-sitosterol and the native ligand. This indicates that both compounds have weaker binding affinities and may not interact optimally with the protein active site. This difference may be attributed to the linear structure and lack of specific interacting groups in fatty acids, resulting in more nonspecific interactions.

The visualization of the docking results in Figure 7 shows that the interaction of β-sitosterol with the target protein is dominated by hydrophobic bonds and van der Waals interactions with key residues in the binding pocket. A more negative binding energy generally indicates greater complex stability, making β-sitosterol potentially more effective than the other two compounds in inhibiting the activity of the target protein. The main interactions formed by the native ligand included hydrogen bonds with the residues HIS A:475, GLU A:305, and ARG A:346, as well as hydrophobic interactions, such as π-alkyl and π-π T-shaped interactions, with aromatic residues such as PHE A:356. These interactions indicate a strong affinity for the protein active site. β-Sitosterol, as a lipophilic compound, exhibited predominantly hydrophobic interactions with residues such as LEU A:298, LEU A:339, MET A:340, ILE A:373, and PHE A:356. Although it did not form hydrogen bonds, these interactions indicate a potentially high affinity due to the involvement of key residues in the active site.

Meanwhile, cis-vaccenic acid formed one hydrogen bond with the residue GLY A:472 and interacted through numerous hydrophobic interactions with residues such as LEU A:298, MET A:336, PHE A:356, and LEU A:380. This indicates that its long alkyl tail is relatively stable in the active site pocket. Hexadecanoic acid, or palmitic acid, exhibited two significant hydrogen bonds with residues GLU A:305 and ARG A:346, as well as several hydrophobic interactions with residues such as PHE A:356, LEU A:298, and MET A:295. This interaction pattern indicates that all three test compounds are capable of occupying the protein active site through various types of interactions, including hydrogen bonding and hydrophobic interactions. However, the strength of these interactions varies depending on the type of ligand and the position of the involved residues, which can affect the overall stability and affinity of the ligand-protein complex.

The docking results indicated that estradiol interacted primarily with residues MET295, LEU476, HIS475, and GLY472, which form the active binding pocket of the EGFR kinase domain. This site is the binding site for natural ligands and specific inhibitors, which play a crucial role in inhibiting receptor phosphorylation. Meanwhile, the compounds identified by GC-MS from *A. ingens*, namely β-sitosterol, cis-vaccenic acid, and hexadecanoic acid, showed varying interaction patterns but remained within the same active region as the control ligand.

β-Sitosterol showed stable interactions with residues MET295, HIS475, and LEU476, as well as involvement of the same residues as estradiol, including GLU305, HIS475, LEU298, MET295, and ALA302. This indicates that β-sitosterol binds to an identical active domain and therefore has the potential to inhibit EGFR activity through a competitive mechanism. Cis-vaccenic acid interacted with residues MET295, PHE356, and GLY472, which were also identified among the estradiol-binding residues. This indicates that this ligand occupies a similar domain, although its orientation is slightly shifted due to the length and flexibility of its aliphatic chain. Consequently, its binding affinity value was lower than that of β-sitosterol. Meanwhile, hexadecanoic acid showed major interactions with residues LEU476, ARG346,

GLY472, and GLU305, with hydrophobic interactions as the dominant bonding force.

Although not all interacting residues were identical to those of the control ligand, the involvement of GLY472 indicates that this compound is still located near the main active site, but with a weaker binding affinity. This difference is related to its smaller molecular size and lack of polar functional groups that can participate in hydrogen bonding [24]. Overall, the results of the interaction domain analysis indicate that the three docked compounds occupy the same active site as, or are located very close to, the control ligand estradiol. The similarity of these interaction domains strengthens the hypothesis that compounds from *A. ingens* have the potential to inhibit EGFR activity through a competitive binding mechanism in the same catalytic region. Thus, these interactions may serve as a potential basis for the development of drug candidates.

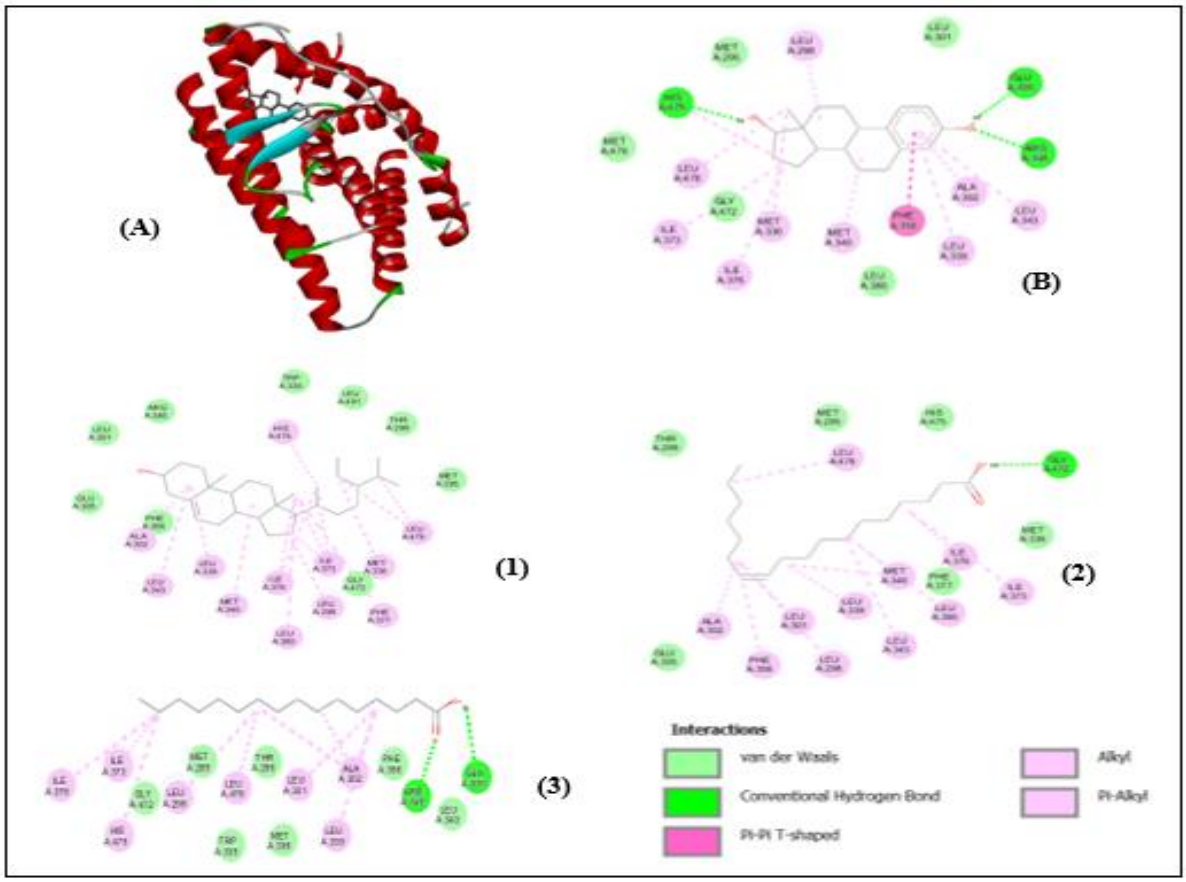

Figure 7. Binding and interaction areas of ligand and protein: (A) 3D protein and ligand; (B) native ligand; (1) β-sitosterol; (2) cis-vaccenic acid; and (3) hexadecanoic acid.

Conclusion

β-Sitosterol was successfully isolated from the *n*-hexane fraction of the sponge *A. ingens* collected from the waters of the Spermonde Archipelago. The toxicity test results showed that the methanol extract was highly toxic, with an LC_{50} value of 24.831 µg/mL. Characterization of isolate I-3 using FTIR showed typical absorption bands corresponding to the functional groups of β-sitosterol, namely O-H stretching, =C-H stretching, C-H stretching, C-H bending, C=C stretching, and C-O stretching. The molecular mass of β-sitosterol was confirmed by GC-MS analysis at 414 g/mol. *In silico* analysis through molecular docking showed a strong

interaction between β-sitosterol and the target protein, with the lowest binding energy of −11.49 kcal/mol. This value indicates the possibility of stable and specific binding, making this compound a promising candidate for anticancer activity.

Acknowledgments

The authors would like to express their gratitude to the Institute for Research and Community Service (LPPM) of Universitas Hasanuddin for funding this research through the PDPU scheme in 2025, under contract number 01260/UN4.22/PT.01.03/2025, dated March 27, 2025.

References

1. Losung, G., Losung, F., Lintang, R. A., Wullur, S., & Manoppo, H. (2022). Aktivitas Antibakteri Dari Spons Asal Perairan Pulau Bantong Bolaang Mongondow Timur. *Jurnal Pesisir Dan Laut Tropis*, *10*(1), 81-88.
2. Handayani, D., & Aminah, I. (2017). Antibacterial and cytotoxic activities of ethyl acetate extract of symbiotic fungi from West Sumatra marine sponge Acanthrongylophora ingens. *Journal of Applied Pharmaceutical Science*, *7*(2), 237-240. doi: 10.7324/JAPS.2017.70234
3. Esposito, G., Mai, L. H., Longeon, A., Mangoni, A., Durieu, E., Meijer, L., ... & Bourguet-Kondracki, M. L. (2019). A collection of bioactive nitrogen-containing molecules from the marine sponge acanthostrongylophora ingens. *Marine drugs*, *17*(8), 472.
4. Ibrahim, S. R., & Mohamed, G. A. (2017). Ingenine E, a new cytotoxic β-carboline alkaloid from the Indonesian sponge Acanthostrongylophora ingens. *Journal of Asian natural products research*, *19*(5), 504-509.
5. Ushiyama, S., Umaoka, H., Kato, H., Suwa, Y., Morioka, H., Rotinsulu, H., ... & Tsukamoto, S. (2012). Manadosterols A and B, sulfonated sterol dimers inhibiting the Ubc13–Uev1A interaction, isolated from the marine sponge Lissodendryx fibrosa. *Journal of natural products*, *75*(8), 1495-1499. doi:10.1021/np300352u
6. Sapar, A., Kurniawan, M. R., Shofiyani, A., Aritonang, A. B., & Setiawan, E. (2022). Sponge Biology Characteristics and Steroids Secondary Metabolite of Haliclona sp. from Lemukutan Island, West Kalimantan, Indonesia. *Asian Journal of Chemistry*, *34*(9), 2373-2378.
7. Vundru, S. S., Kale, R. K., & Singh, R. P. (2013). β-sitosterol induces G1 arrest and causes depolarization of mitochondrial membrane potential in breast carcinoma MDA-MB-231 cells. *BMC complementary and alternative medicine*, *13*(1), 280.
8. McLaughlin, J. L., Rogers, L. L., & Anderson, J. E. (1998). The use of biological assays to evaluate botanicals. *Drug information journal*, *32*(2), 513-524.
9. Klimoszek, D., Jeleń, M., Dołowy, M., & Morak-Młodawska, B. (2024). Study of the lipophilicity and ADMET parameters of new anticancer diquinothiazines with pharmacophore substituents. *Pharmaceuticals*, *17*(6), 725. doi: 10.3390/ph17060725
10. Nhlapho, S., Nyathi, M. H. L., Ngwenya, B. L., Dube, T., Telukdarie, A., Munien, I., ... & Chude-Okonkwo, U. A. K. (2024). Druggability of pharmaceutical compounds using Lipinski rules with machine learning. *Sci. Pharm*, *3*(4), 177-192. doi: 10.58920/sciphar0304264
11. Lau, V., Nurkolis, F., Park, M. N., Heriyanto, D. S., Taslim, N. A., Tallei, T. E., ... & Kim, B. (2024). Green seaweed Caulerpa racemosa as a novel non-small cell lung cancer inhibitor in overcoming tyrosine kinase inhibitor resistance: An analysis employing network pharmacology, molecular

docking, and in vitro research. *Marine Drugs*, *22*(6), 272. doi: 10.3390/md22060272

12. Wulandari, R. P., Gabriel, K., Nurdin, H. A., Pakhrul, D. H. F., Harits, S. S., Prameswari, N., ... & Aulifa, D. L. (2023). In silico study of secondary metabolite compounds in parsley (Petroselinum crispum) as a drug therapy for blood cancer (myeloproliferative neoplasm (MPN)) targeting JAK-2. *Indonesian Journal of Chemical Science*, *12*(2), 212-224.
13. Asha. R, Sundara Prabha. V and Beschi A. R. (2022). Admet Analysis, Biological Activity and Target Protein Prediction Studies of the Selected Phytocompounds Using Online Tools. *International Journal of Pharmaceutical Research and Applications*, 7(3), pp: 2049-2055
14. Chandramouli, M., & Surendra, M. H. (2025). Pharmaceutical Innovation Through Computational Drug Design: A Comprehensive Exploration. *Makara Journal of Science*, *29*(2), 6. doi: 10.7454/mss.v29i2.2629
15. Rajput, D., Jain, D., Kashaw, S. K., & Patil, U. K. (2024). Molecular Docking Studies on Phytoconstituent Isolated from Nyctanthes arbortristis Linn. *International Journal of Pharmaceutical Investigation*, *14*(2).
16. Rasyid, H., Asmirah, A., Firdausiah, S., Arief, I., & Soekamto, N. H. (2024). The potential of Paku Gajah (Angiopteris evecta) as antitumor through in vitro and in silico studies. *Molekul*, *19*(2), 296-308. doi: 10.20884/1.jm.2024.19.2.10644
17. Thakur, M., Kumari, S., Kumar, S., & Kumari, M. (2024). Integrated quantum chemical calculations, predictive toxicity assessment, absorption, distribution, metabolism, excretion and toxicity profiling and molecular docking analysis to unveil the therapeutic potential of non-oxovanadium (IV) and organotin (IV) complexes targeting breast cancer cells. *International Journal of Quantum Chemistry*, *124*(13), e27438
18. Firdausiah, S., Firdaus, F., Sulaeha, S., Rasyid, H., & Amalia, S. F. (2023). Citronella extracts: Chemical composition, in vivo and in silico insecticidal activity against fall armyworm (Spodoptera frugiperda JE Smith). *Egyptian Journal of Chemistry*, *66*(7), 235-243. doi: 10.21608/EJCHEM.2022.147926.6441
19. Wahyuni, D. K., Rahmawati, C. T., Syukriya, A. J., Dismayanti, N., Arifin, M. B., Kharisma, V. D., ... & Prasongsuk, S. (2025). Metabolite characterization and in vitro antiplasmodial potential assessment of Sonchus arvensis L. callus under glutamine treatment. *Scientific Reports*, *15*(1), 35956. doi: 10.1038/s41598-025-12617-z
20. Shehroz, M., Aslam, M., Khan, M. A., Aiman, S., Afridi, S. G., & Khan, A. (2019). The in silico characterization of a salicylic acid analogue coding gene clusters in selected Pseudomonas fluorescens strains. *Iranian Journal of Biotechnology*, *17*(4), e2250. doi: 10.30498/ijb.2019.95299
21. Belal, A. (2018). Drug likeness, targets, molecular docking and ADMET studies for some indolizine derivatives. *Die Pharmazie-An International Journal of Pharmaceutical Sciences*, *73*(11), 635-642. doi: 10.1691/ph.2018.8061
22. Agu, P. C., Afiukwa, C. A., Orji, O. U., Ezeh, E. M., Ofoke, I. H., Ogbu, C. O., ... & Aja, P. M. (2023). *Molecular docking as a tool for the discovery of molecular targets of nutraceuticals in diseases management. Sci Rep. 2023; 13: 13398*. doi: 10.1038/s41598-023-40160-2
23. Prabawati, S. Y., Triatmaja, K., & Widiakongko, P. D. (2025). Molecular Docking Study of Eugenol and Its Derivatives as Potential Anti-Ischemia Agents for Angiotensin Converting Enzyme (ACE) Inhibition. *Indonesian*

Journal of Chemistry, *25*(3), 929–942. doi: 10.22146/ijc.101791.

24. Carpenter, K. A., & Altman, R. B. (2024). Databases of ligand-binding pockets and protein-ligand interactions. *Computational and Structural Biotechnology Journal*, *23*, 1320-1338. doi: 10.1016/j.csbj.2024.03.015